Journal of Molecular Structure 1168 (2018) 127–134

Contents lists available at ScienceDirect

Journal of Molecular Structure

journal homepage: http://www.elsevier.com/locate/molstruc

Cyanocyclohexane: Axial-to-equatorial "seesaw" parity in gas and condensed phases

Tran Dinh Phien [a], Liubov E. Kuzmina [b], Ágúst Kvaran [c], Sigridur Jonsdottir [c], Ingvar Arnason [c], Sergey A. Shlykov [b, *]

[a] Institute of Research and Development, Duy Tan University, 03 Quang Trung, Da Nang, Viet Nam
[b] Department of Physical and Colloidal Chemistry, Ivanovo State University of Chemistry and Technology, Research Institute for Thermodynamics and Kinetics of Chemical Processes, 7 Sheremetievskiy Ave, 153000, Ivanovo, Russian Federation
[c] Science Institute, University of Iceland, Dunhaga 3, IS-107, Reykjavik, Iceland

ARTICLE INFO

Article history:
Received 1 April 2018
Received in revised form
4 May 2018
Accepted 4 May 2018
Available online 7 May 2018

Keywords:
Cyanocyclohexane
Gas-phase electron diffraction
Dynamic NMR
Quantum chemical calculations
Equatorial-to-axial equilibrium
Molecular structure

ABSTRACT

Conformational properties and molecular structure of cyanocyclohexane **1** were studied by gas-phase electron diffraction (GED) and dynamic NMR as well as by detailed quantum chemical (QC) computations. This compound violates the so called 'equatorial rule' according to which the substituents attached to one of the carbon atom of the ring prefers to occupy an equatorial position relative to the frame of cyclohexane. In case of **1**, both conformers contribute nearly equally in gas and liquid phases, with slight domination of the equatorial form as found from the experimental data, Eq:Ax of ca. 3:2. The QC calculations predict contradictive conformer preference depending on method/basis set combination applied. Enthalpy and entropy contributions to Eq↔Ax equilibrium are analyzed.

1. Introduction

Saturated six-membered cyclic compounds are widely used in pharmaceutics, chemistry, are part of a number of food products, polymers and dyes. For this reason, their structures extensively in various phases are widely studied, see, for example, [1,2].

Physicochemical behavior of these compounds is essentially dependent on a heteroatom(s) embedded into the cycle, such as piperidines [3,4], tetrahydropyrans [5,6], silacyclohexanes [7,8], etc. Another property-modifying factor is substitution of a hydrogen atom by another atom or group of atoms R (R = halogen [9], alkyl [10], alkenyl or aromatic radicals [11], methoxy [12], etc.). In this case, an alternative occurs for the substituent to occupy either equatorial or axial position relative to the cycle. The identification of the laws of equatorial-axial equilibrium in the derivatives of saturated six-membered heterocyclic compounds is a valuable information on the nature of steric and orbital interactions in organic molecules.

The conformational axial-equatorial equilibrium of cyanocyclohexane NC–C_6H_{11} 1 was studied by microwave spectroscopy, Raman scattering in liquid, IR spectroscopy in the Xe matrix, NMR spectroscopy, and quantum chemical calculations [13–16]. It is to be noted that the published results indicate some dominance of either one or another conformer (equatorial or axial), depending on the method applied. In the case IR spectroscopy, in the Xe matrix at a temperature 218–173 K, $\Delta H = -0.18$ (3) kcal/mol, and the ratio $X_{Eq}:X_{Ax} = 42(8):58(8)\%$ was evaluated for ambient temperature; the enthalpy of $\Delta H = -0.13$ (5) kcal/mol obtained from Raman data in the liquid at 296–333 K coincide with the IR results [13]. The opposite situation is observed in NMR spectroscopy of 1 in CCl_4, $X_{Eq}:X_{Ax} = 54.5 \pm 1.7:45.5 \pm 1.7\%$ at 303 K [14], from which we estimated ΔG (303 K) = 0.11 (8) kcal/mol.

Quantum chemical calculations (QC) for gas phase also give contradictory data for the ΔE values: 0.52 (B3LYP), −0.73 to −0.34 (MP2), with 6-311 + G** or 6-311G** basis sets [13], and −0.15 (M06-2X/aug-cc-pVTZ) and ΔG (298 K) = −0.06 kcal/mol [15]. It is important to note that only ΔE values are given in Ref. [13], but not ΔG which determines the conformer ratio. A microwave (MW) study performed in Ref. [13] at ambient temperature provided with

* Corresponding author.
E-mail address: shlykov@isuct.ru (S.A. Shlykov).

https://doi.org/10.1016/j.molstruc.2018.05.013
0022-2860/

structural information on the conformers of gaseous 1 though no evident information on the axial-to-equatorial ratio is recommended.

In this work, we represent the results of combined gas-phase electron diffraction/mass-spectrometric (GED/MS) study along with QC calculations which provides with the first experimental data on conformational axial-equatorial equilibrium in the gas phase. This study is also of interest in connection with the fact that this particular substituent, a carbonitrile group, has a significant effect on the conformational equilibrium due to a strong conjugation. Comparison of the structural and conformational properties of 1 with our recent results on 1-cyano-1-silacyclohexane [15], N-cyanopiperidine and 1-cyanophosphorinane [17] may clarify tendencies in the series of the 1-heterocyclohexanes. We also present a dynamic NMR study, which allows us to measure the frozen conformational equilibrium and obtain thermodynamic parameters like the free energy of activation. In addition, a detailed exploration of the cycle inversion potential energy surface of 1 was carried out for the axial-to-equatorial transition, and more sophisticated, that in earlier works, calculations taking into account dispersion interactions, such as B3LYP-D3, were applied.

2. Experimental

2.1. GED-MS experiment

A sample of cyanocyclohexane was purchased from Sigma-Aldrich Chemical Company, 98%, and used without further purification. The diffraction patterns were recorded during a combined gas-phase electron diffraction and mass-spectrometric experiment carried out using the EMR-100/APDM-1 unit [18,19].

The sample of the cyanocyclohexane was evaporated from a molybdenum cell with a cylindrical effusion nozzle of $0.6 \times 1.2\ mm^2$ size (diameter x length) at 297 (3) K. The conditions of the GED/MS experiment and data refinement details are given in Supporting Information.

Mass spectra (EI, 50 eV) of the effusing molecular beam were recorded simultaneously with the collection of the diffracted electrons. The mass spectrum is in good agreement with the NIST data [20].

2.2. NMR experiment

A 400 MHz NMR spectrometer (Bruker Avance 400) was used for all NMR experiments. Toluene-*d*8 was used as solvent for the low-temperature ^{13}C NMR measurements. The temperature of the probe was calibrated by means of a type K (Chromel/Alumel) thermocouple inserted into a dummy tube. The readings are estimated to be accurate within ±2 K. The NMR spectra were loaded into the data-handling program IGOR (WaveMetrics) for analysis, manipulations, and graphic display. Line shape simulations of the NMR spectra were performed by using the WinDNMR program [21].

2.3. Computational details

Quantum chemical (QC) calculations of the cyanocyclohexane conformers were performed with the use of the Gaussian 09 program system [22].

In this paper, the geometry and vibrational calculations were performed using DFT (with B3LYP, B3LYP-D3, where an empirical dispersion correction has been added, and M062X functionals) and MP2 methods with the 6-311G** and cc-pVTZ basic sets.

Geometry optimizations of the axial and equatorial conformers were performed under C_s symmetry. Calculated relative energies and free Gibbs energies along with the equilibrium population of these conformers in the gas phase at room temperature are summarized in Table 1.

Potential energy surface (PES) of the ring conversion was obtained by synchronous scanning two opposite dihedral angles of the ring at M062X/6-311G** level.

Lowest energy pathway for the *axial-to-equatorial* interconversion of the cyanocyclohexane was calculated with the use of the quadratic synchronous transit approach (Synchronous Transit-Guided Quasi-Newton – STQN) [23,24] method with keywords QST2 and PATH at M062X/aug-cc-pVTZ level.

Chemical shift calculations were performed using the gauge-independent atomic orbital (GIAO) method [25]using ORCA 4.0 [26]on the RI-MP2/def2-TZVP geometries at the PBE0 level of theory [27]and using the pcSseg-2 basis set [28]on carbon atoms and def2-TZVP on other atoms [26]. Tetramethylsilane was used as a computational reference for converting calculated shieldings into chemical shifts.

3. Results and discussion

3.1. Energies

The geometry and vibrational calculations for **1** were performed using DFT (with B3LYP, B3LYP-D3 and M062X functionals) and MP2 methods with the 6-311G** and cc-pVTZ basic sets. Theoretical relative total energy, free Gibbs energy, and the molar fraction of the conformers are summarized in Table 1. Experimental values of ΔG, ΔH and conformer contributions are compiled in Table 2.

All calculations performed show the axial and equatorial conformers to coexist in gas phases at room temperature, both possessing a C_s equilibrium symmetry, Fig. 1. However, the conformational ratios are predicted in different way. The DFT methods in combination with both, B3LYP and B3LYP-D3, functionals resulted in the relative Gibbs energies from ca. 0.3–0.7 kcal/mol that corresponds to some domination of the Eq conformer, 59–77 mol.%. The two basis sets, 6-311G** and cc-pVTZ, applied with the M06-2X functional yielded slightly opposite estimates, 41 and 51 mol.%, respectively. At the same time, all the second order perturbation theory calculations coincide in an axial conformer preference, 60–70 mol.%. More sophisticated calculations, coupled cluster with complete basis set extrapolation, performed by Belyakov et al. [15], show a trend similar to that from the DFT method, and best agreement is with the one which takes into

Table 1
Relative total electron energies ΔE, free Gibbs energies ΔG for the Eq↔Ax interconversion) of cyanocyclohexanes from QC calculations.

QC calculations	ΔE	ΔG	X_{Eq}:X_{Ax}
B3LYP/6-311G**	0.41	0.57	72:28
B3LYP/6-311 + G**	0.52[a]		
B3LYP/cc-pVTZ	0.57	0.72	77:23
B3LYP-D3/6-311G**	0.03	0.26	59:41
B3LYP-D3/cc-pVTZ	0.21	0.38	66:34
M06-2X/6-311G**	−0.56	−0.21	41:59
M06-2X/cc-pVTZ	−0.33	0.02	51:49
M06-2X/aug-cc-pVTZ[b]	−0.15	−0.06	47:53[c]
MP2(FC)/6-311G**	−0.73[a]/-0.69	−0.40	34:66
MP2(FC)/cc-pVTZ	−0.43		
MP2(FC)/6-311 + G**	−0.49[a]/−0.45	−0.28	38:62
MP2(Full)/6-311 + G**	−0.34[a]/−0.49	−0.32	37:63
CCSD(T)/CBS + therm.corr	0.03[b]	0.16[b]	57:43[c]

[b] Calculated in this work from the X_{Eq}:X_{Ax} ratio [15].
Data from: [a] [13], [b] [15].
[c] Calculated in this work from ΔG value [15].

Table 2
Relative Gibbs free energies ΔG, enthalpies ΔH (kcal/mol) and equatorial: axial ratio for the Eq↔Ax interconversion of **1** as derived from experimental studies.

Method	Solvent (*T*)	ΔG	X_{Eq}:X_{Ax}	Ref.
IR	Xe (173–218 K)	(ΔH) −0.18 (3)	42(8):58(8)[a]	[13] [a]
Raman	Neat liquid ((296–333 K)	(ΔH) −0.13 (5)	45:55[a]	[13]
NMR	*t*-C_4H_9OH (339 K)	0.25	59:41[b]	[30] [c]
NMR	*t*-C_4H_9OH (298 K)	0.15	56:44[b]	[31] [c]
NMR	CS_2 (194 K)	0.24	65:35[b]	[16] [d]
NMR	CCl_4 (303 K)	0.11 (8)[h]	54.5(31):45.5(31)	[14] [e]
NMR	$CFCl_3$ (178 K)	0.21	64:36[b]	[32] [f]
NMR	$CFCl_3$ (194 K)	0.18	61:38[b]	[33] [g]
NMR	Toluene-d_8 (227 K)	0.24	63:37	This work
GED	Gas (287 K)	0.28 (19)	62(8):38(8)	This work

[a] Calculated from ΔH values under the assumption that the −TΔS term has a small contribution to ΔG.
[b] Calculated in this work from ΔG values of the corresponding cited references.
[c] Base catalyzed equilibrium of the *cis* and *trans* isomers of 4-*t*-butylcyclohexyl cyanide.
[d] Integration of the areas under the axial and equatorial methine proton resonances.
[e] Conformational analysis using lanthanide-induced shifts (^{1}H NMR).
[f] Integration using ^{13}C NMR.
[g] Dynamic ^{1}H NMR studies of three-spin systems in 1-substituted cyclohexanes-2,2,3,3,4,4,5,5-d_8.
[h] Calculated in this work from the X_{Eq}:X_{Ax} ratio of the corresponding cited references.

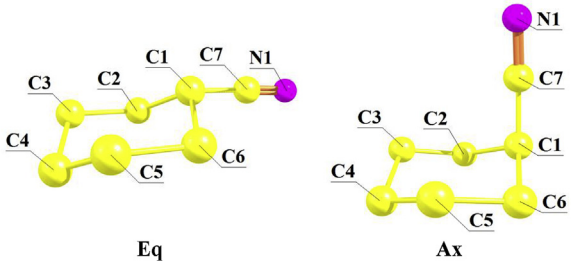

Fig. 1. Conformers of Cyanocyclohexane with atom numbering.

account the dispersion interactions, recommended by Grimme et al. [29], B3LYP-D3/6-311G**.

3.2. Internal inversion

It is well known that for cyclohexane derivatives the axial-to-equatorial and backward transformations are normally pass by ring inversion via one or several intermediate structures. In the first step, the ring inversion potential energy surface (PES) profile of **1** was explored by scanning it at fixed C1–C2–C3–C4 dihedral angle at the M062X/6-311G** and M062X/aug-cc-pVTZ levels with a step size of 10°, see Fig. S1. When starting from nearly axial conformer (black line) (∠C1–C2–C3–C4 ≈ −70°), the scan transformed the molecule to an almost *half-twist* shape of the ring I (∠C1–C2–C3–C4 ≈ 10° and ΔE ≈ 12 kcal/mol) followed by an energy and structure 'jump' and then another jump of structure to a *boat*-like shape II at *ca.* 50°, 7 kcal/mol. Almost identical route takes place when starting from the equatorial conformer (red line).

A much 'smoother' PES was obtained by synchronous scanning two opposite dihedral angles of the ring, C1–C2–C3–C4 and C1–C6–C5–C4 (Fig. 2). The intermediate minima between axial and equatorial forms correspond to twist structures.

In the third step, the energy pathway for the equatorial-to-axial interconversion ofCNP was calculated using the quadratic synchronous transit approach (Synchronous Transit-Guided Quasi-Newton – STQN) method with keywords QST2 and PATH at M062X/aug-cc-pVTZ level, Fig. 3. Two sets of calculations were performed: axial-to-twist and twist-to-equatorial. Transition states, optimized by QST2 calculations, appeared to be *half-twist* with the energies about 13 kcal/mol above the most stable, axial

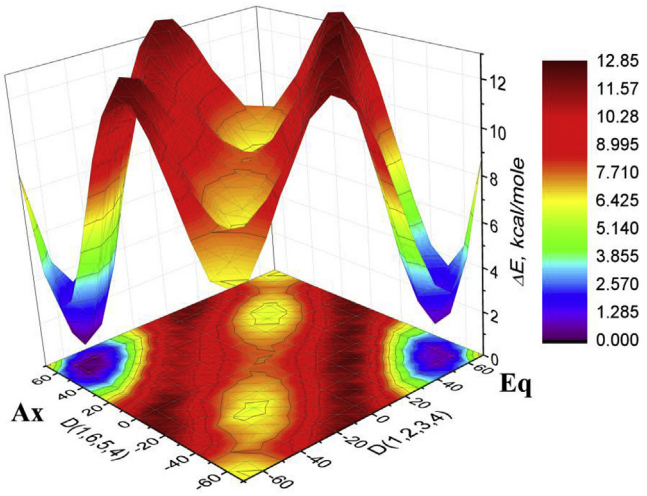

Fig. 2. 3-D presentation of the relative energy surface of thecyanocyclohexane molecule calculated at the M062X/6-311G** level of theory, shown as a function of two dihedral angles.

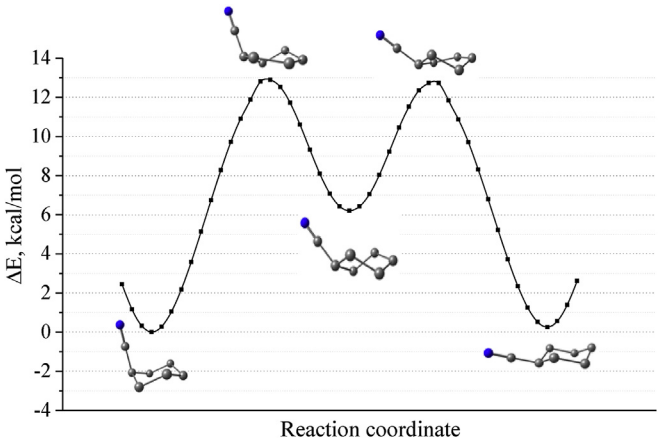

Fig. 3. Lowest energy pathway for the axial-to-equatorial interconversion of the cyanocyclohexane molecule calculated by the STQN method at the M062X/aug-cc-pVTZ level of theory and molecular models for minima and transition states.

and equatorial, forms and *ca.* 6 kcal/mol above the twist conformation.

3.3. GED analysis

The molecular structure of both conformers of **1** with atom numbering is shown in Fig. 1. The following independent geometric parameters were used to describe the geometry of the axial conformer: bond distances C1–C2, C1–C7, N1≡C7 and H1–C1; bond angles C2–C1–C6, C6–C1–C7, C1–C7–N1, C6–C1–H1, dihedral angle C3–C2–C1–C6. For the both conformers, the C_s symmetry was fixed as found in the QC calculations. All other geometrical parameters for the both conformers were described by the parameters analogous to those in the axial conformer and corrected by adding the differences taken from MP2/6-311G** calculations.

Vibrational amplitudes for the both conformers were refined insix groups according to the specific regions in the radial distribution, see Fig. 4: 0–1.3, 1.3–1.8, 1.8–3.2, 3.2–4.5, 4.5–6.0, 6.0–8.0 Å. The vibrational corrections Δr and starting values of amplitudes were calculated by the Vibmodule program [34] using the so called second approximation, in which harmonic approach with nonlinear relation between Cartesian and internal coordinates were applied on the base of the force field estimated in the quantum chemical calculations at MP2/6-311G** level, Table S1 in Supporting material.

In course of the least-squares (LS) analyses, the relative contributions of the conformers were refined along with the geometric and vibrational parameters and converged at $X_{Eq}:X_{Ax} = 62(5):38(5)\%$, where the uncertainty is given as $3\sigma_{LS}$. In additions, refinements were performed at fixed contributions, and from the plot of the agreement factor R_f vs X_{Ax} (Fig. S2) an uncertainty was derived to be ±8 mol. % according to Hamilton's criterion. Thus, a conformational ratio value from the GED data is recommended as $X_{Eq}:X_{Ax} = 62(8):38(8)\%$ in gas phase at 287 K which corresponds to ΔG (287 K) = 0.28 (19) kcal/mol.

Theoretical, for the refined conformer mixture, and experimental radial distribution f(r) curves and molecular scattering functions sM(s) along with the differences "Exp-Theor" are given in Figs. 4 and 5, respectively. Theoretical and experimental geometric parameters of **1** are compiled in Table 3.

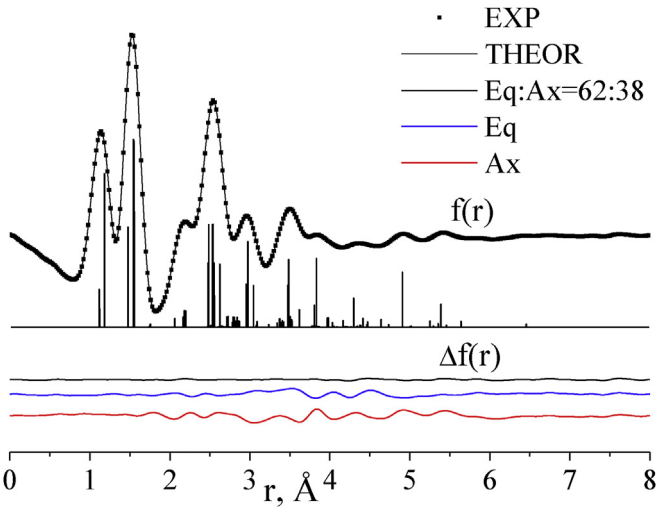

Fig. 4. Experimental (dots) and theoretical (line) radial distribution curves f(r) for refined conformer mixture. Differences Δf(r) "Experim.–Theor." are given at the bottom; colored lines correspond to refinement of all parameters under assumptions of the individual conformers.

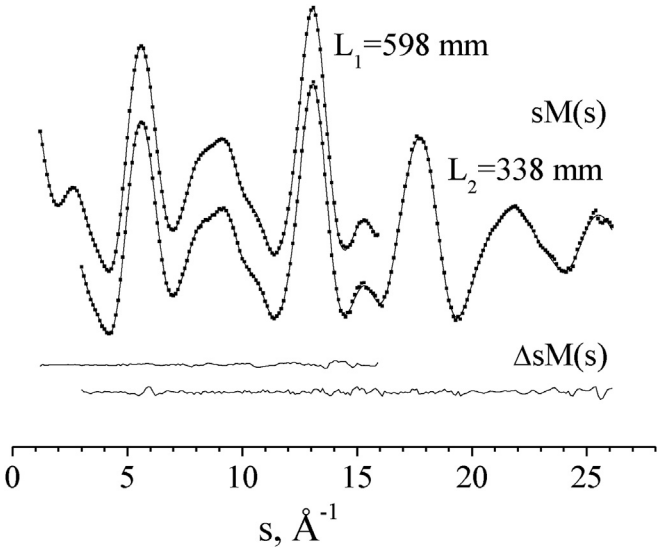

Fig. 5. Theoretical (line) for the refined conformer mixture and experimental (dots) molecular scattering intensities sM(s); differences ΔsM(s) "Experim.–Theor." are given at the bottom.

3.4. Geometrical parameters

The endocyclic C–C bond lengths are better predicted by the DFT method than by MP2 as compared with the GED results, see Table 3. The C–H distances are 0.01 Å longer from the GED experiment than from the QC calculations. The triple C≡N bond is by 0.022–0.026 Å underestimated from the density functional calculations.

For the exocyclic C1–C7 bond all the applied methods yielded an excellent prediction; its length of 1.465 Å is noticeably shorter than the 'classical' ordinary C–C bond, see the endocyclic ones of ca. 1.54 Å, due to influence of the cyano group, but still longer than the sesquialteral bond of ca. 1.40 Å. Similar shortening of a bond adjacent to the C≡N group was observed for N–cyanopiperidine [17]. On the other hand, the case of 1-cyano-silacyclohexane [15] is somewhat uncertain: according to the M062X/aug-cc-pVTZ calculations, the r (Si–C7)/r (Si–C2) values are 1.875/1.867 and 1.869/1.867 Å for axial and equatorial forms, respectively, i.e. predicting the exocyclic bond to be longer for axial position of the substituent. Additional calculations performed in Ref. [15] for 1-cyano-silacyclohexane showed same result for when augmentation of the basis set was not applied at M062X approach, while all other calculations, B3LYP, B3LYP-D3 and MP2 in combination with different basis sets (6-311G**, cc-pVTZ and aug-cc-pVTZ) predict the exocyclic Si–C bond to be ca. 0.01 Å shorter that its endocyclic counterpart.

Theoretical bond angles are in excellent agreement with the GED values. An exception occurs in case of the C1C7N angle: very small, less than 2°, deviation from flat angle (QC) versus 13±2° (GED), towards *cis* orientation relative the C2C1C6 plane. Same trend was found for N–cyanopiperidine [17] and is probably due to 'shrinkage' effect inherent to the GED data, not completely compensated by vibrational corrections in harmonic approximation applied, see section GED analysis.

The substituent is strictly parallel to the cyclohexane frame, but deviates from perpendicularity by 10 to 14° towards *cis* orientation relative the C2C1C6 plane in the equatorial and axial conformers, respectively (see α angles in Table 3). No influence of the cyano

Table 3
Theoretical (with 6-311G** basis set) and experimental geometric parameters[a] of **1**.

Conformer	Equatorial				Axial				Equatorial/Axial
Method	B3LYP-D3	M062X	MP2	GED[e]	B3LYP-D3	M062X	MP2	GED[e]	MW[d]
Bond distance, Å									
C1–C2	1.547	1.539	1.534	1.546 (3)	1.549	1.541	1.542	1.548 (3)	1.544(3)/1.544(3)
C1–C7	1.463	1.465	1.465	1.465 (3)	1.467	1.469	1.468	1.468 (3)	1.464(3)/1.470(3)
C7≡N1	1.153	1.149	1.175	1.175 (2)	1.153	1.149	1.176	1.176 (2)	1.161(3)/1.162(3)
C2–C3	1.534	1.529	1.531	1.537 (3)	1.534	1.529	1.531	1.537 (3)	1.532(3)/1.532(3)
C3–C4	1.535	1.530	1.531	1.537 (3)	1.536	1.531	1.532	1.538 (3)	1.536(3)/1.536(3)
C2-H_{Ax}	1.096	1.095	1.098	1.110 (2)	1.096	1.095	1.098	1.110 (2)	1.090(3)/1.090(3)
C2-H_{Eq}	1.093	1.092	1.095	1.108 (2)	1.093	1.092	1.095	1.108 (2)	1.087(3)/1.087(3)
Bond angle, °									
C1C2C3	110.7	110.4	110.5	110.5 (3)	111.8	111.4	111.2	111.2 (3)	110.2(5)/111.4(5)
C2C3C4	111.6	111.3	111.2	110.7 (3)	111.4	111.1	111.0	111.0 (3)	110.8(5)/111.6(5)
C3C4C5	111.3	111.1	110.9	109.8 (3)	111.5	111.2	111.3	111.3 (3)	110.9(5)/111.1(5)
C2C1C6	111.1	111.1	110.9	110.9 (3)	110.6	110.8	110.5	110.5 (3)	110.9(5)/110.5(5)
C2C1C7	111.2	110.6	110.7	110.7 (4)	110.7	110.0	109.9	109.9 (4)	110.8(5)/110.0(5)
C1C7N1	178.9	178.7	178.5	167.2 (15)	178.8	178.5	178.3	167.0 (15)	179.0(5)/178.8(5)
Torsion angle, °									
C1C2C3C4	−55.6	−56.1	−56.4	−56.4 (19)	−55.1	−55.7	−56.0	−56.0 (19)	−56.9(10)/-55.6(10)
C2C3C4C5	55.4	56.1	56.4	56.4 (19)	55.2	56.0	55.9	55.9 (19)	
α[b]	0.1	0.2	0.1	0.7	79.4	77.3	76.4	76.4	
Flap (C1)[c]	50.6	51.3	51.3	51.1	49.0	49.8	50.4	50.7	
Flap (C4)[c]	49.9	50.6	51.0	51.0	49.9	50.7	50.6	50.6	

[a] See Fig. 1 for atom numbering; r_e and $\angle_e$ for QC and r_{h1} and $\angle_{h1}$ for GED values are given. r_{h1} values ($r_{h1} = r_a + \Delta r$) are given for GED results. The vibrational corrections Δr and starting amplitudes were calculated by the Vibmodule program [33] using the so called second approximation, in which harmonic approach with nonlinear relation between Cartesian and internal coordinates were applied on the base of the force field estimated in the quantum chemical calculations at MP2/6-311G** level.
[b] α is an angle between the C1–C7 bond and the cyclohexane ring planar frame C2C3C5C6; dependent parameter.
[c] Flap (C1) and Flap (C4) are angles between the C2–C3···C5–C6 plane and the C1–C2–C5 and C4–C3–C5 planes, respectively; dependent parameters.
[d] Microwave r_0 values [13] for the Eq/Ax conformers.
[e] Values in parentheses for the GED data are full errors estimated as $\sigma(r_{h1}) = [\sigma^2_{scale} + (2.5\sigma_{LS})^2]^{1/2}$, where $\sigma_{scale} = 0.002r$ and σ_{LS} is a standard deviation in least-squares refinement for internuclear distances and as $3\sigma_{LS}$ for angles. The place-value is such that the last digit of the uncertainty lines up with the last digit of the nominal value.

group on the flap angle was found, as follows from equality of the flaps at C1 and C4.

Comparison of the two sets of experimental data, MW [13] and GED, shows a good coincidence of the bond lengths within the experimental uncertainties, except C7≡N1 and C–H which are 1% longer from GED, however, the MW value r (C7≡N1) = 1.161 (3) Å is intermediate between DFT and MP2 predictions while the one from GED perfectly reproduces the perturbation theory data. As for the bond and torsion angles, the only discrepancy occurs for the ∠C1C7N1 value which is practically flat from MW, and the smaller value from GED was discussed above in this section.

Experimental root mean square vibrational amplitudes refined in groups as described in Structural analysis section are in acceptable agreement with theoretical predictions, see Table S1. Experimental molecular scattering intensities sM(s) are given in Table S2 in Supporting material.

3.5. Dynamic NMR spectroscopy (DNMR)

The ^{13}C NMR spectra of **1** were recorded in the temperature range of 188–296 K. Toluene-*d*8 was used as solvent. At ambient temperature (296 K) the spectrum is in agreement with a rapid interconversion of the two chair forms. At 243 K all signals show considerable line broadening and on further cooling the line broadening increases and gradual splitting of signals into a main signal and a smaller one occurs, indicating a mixture of a major and a minor conformer. As a general rule in cyclohexane chemistry, the resonance signals of the axial conformer are shifted to lower δ values [35–38]. This effect is most pronounced for the C3 and C5 atoms and less so for C2 (6) and C1 atoms. For C4 the shifting effect similar in magnitude as for C1 but reversed in sign (axial conformer shifted to higher δ values; see Fig. 6). The CN substituent (not shown in Fig. 6) also shows signal splitting (see Supporting material). QC calculations of the chemical shifts, which are a useful tool

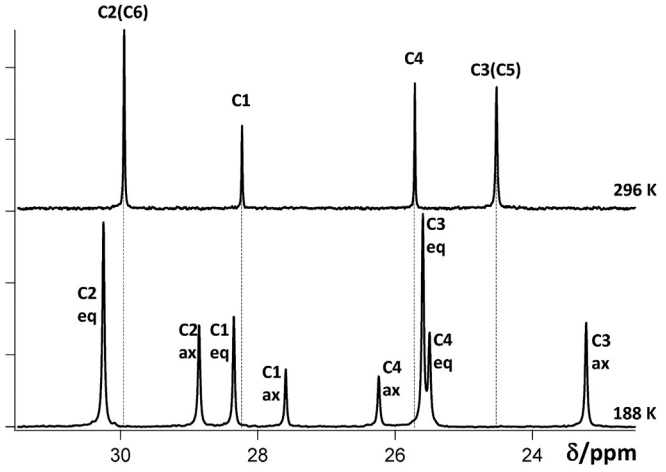

Fig. 6. ^{13}C NMR spectrum of cyanocyclohexane at 296 K (above) and 188 K (below).

for the assignment of chemical shifts to individual atoms, have been used to underline the assignments shown in Fig. 6. See also Table S3 in Supporting material. Based on these observations the major component is assigned to the equatorial conformer.

Based on the signal assignments, dynamic NMR simulations of the CN and C2 (6) signals using the software WinDNMR [21] determination of the rate constants ($(k_{e\rightarrow a})$) and the corresponding free energies of activation ($\Delta G^{\#}_{e\rightarrow a}$) as a function of temperature was allowed. Chemical shifts, derived from NMR spectra, which were recorded at the lowest temperatures, were assumed to represent conditions of negligible interconversions. An average value of $\Delta G^{\#}_{e\rightarrow a} = 10.9 \pm 0.1$ kcal mol^{-1} was obtained for the temperature range 185–245 K. Furthermore, the equilibrium constant ($K_{e\rightarrow a}$) and the free energy difference ($\Delta G_{e\rightarrow a}$), for the

equatorial to axial transformations, corresponding to 227 K (a temperature close to the coalescence point) were determined from the relative signal intensities ($K_{e\rightarrow a} = 0.56$ and $\Delta G_{e\rightarrow a} = 0.26$ kcal mol^{-1}). This corresponds to about 64/36 mol % mixture of the equatorial and axial conformers. Further details are given in the Supporting material.

3.6. Analysis of conformers contribution and thermodynamic parameters for Eq↔Ax equilibrium from theory and experiment

Various QC calculations and experiments show somewhat contradictive results concerning the conformer ration in liquid and gaseous phases of **1**, see Tables 1 and 2. For gas phase at room temperature, the conformer ratio Eq:Ax is predicted to be 3:2 to 3:1 (DFT/B3LYP), 3:2 to 2:3 (DFT/M06-2X), 3:2 to 2:1 (MP2) and 4:3 (CCSD(T)/CBS).

The GED result of this work, ~3:2, demonstrate best fit with that derived from B3LYP-D3 calculations. The NMR data [14,16], though for solution, support the gas phase GED data of some preference of the equatorial form. On the other hand, the IR spectroscopy data of **1** isolated in Xe matrix [13] resulted in opposite ratio, or, within the experimental uncertainties, close to 1:1.

We estimated the temperature-dependence of the conformer ratio. Based on the relative electronic energies and vibrational characteristics obtained from the QC calculations, we calculated the equilibrium constants of the process Eq↔Ax at different temperatures from 100 to 1000 K with a 50 K step using the programs TDF and KP-IZ (by Dr. V.V. Sliznev) at 'rigid rotator-harmonic oscillator' approximation. The results along with experimental data are plotted in Fig. 7. It is clearly seen that the B3LYP functional based calculations show a tendency of the axial form to increase the contribution upon the temperature raise, but to decrease in cases of M06-2X and MP2. As temperature decrease, domination of one of the conformers, depending on the theoretical approach, tends to become absolute. From the experimental temperature-dependent vibrational spectroscopy data [13], the conformational equilibrium shifts towards the Eq form with the temperature increase, since the enthalpies are negative: ΔH = −0.18 (3) IR in Xe and −0.13 (5) kcal/mol Raman in liquid. This coincides with the M06-2X and MP2 estimates.

In addition, we analyzed enthalpy and entropy contributions to the Gibbs ΔG_{298} energies, Fig. 8. From all the calculations performed, entropy decreases for the Eq → Ax process, and the TΔS

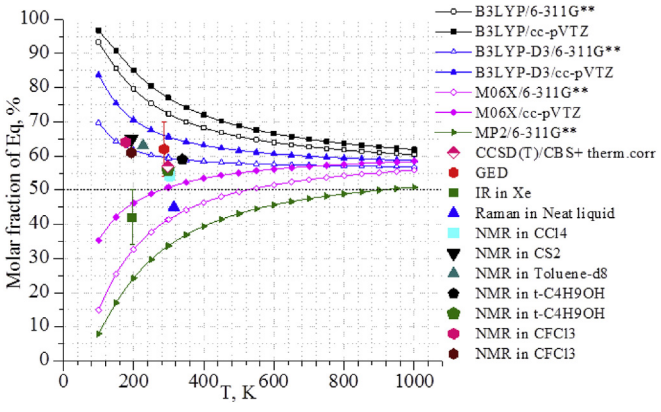

Fig. 7. Temperature dependence of conformer contribution estimated on a basis of quantum chemical calculations along with experimental data IR in Xe and Raman in Neat liquid [13], NMR in CCl_4 [14], NMR in CS_2 [16], NMR in *t*-C_4H_9OH (298 K) [31], NMR in *t*-C_4H_9OH (339 K) [30], NMR in $CFCl_3$ (178 K) [31], NMR in $CFCl_3$ (194 K) [32], DNMR in toluene-*d*8 and GED (this work).

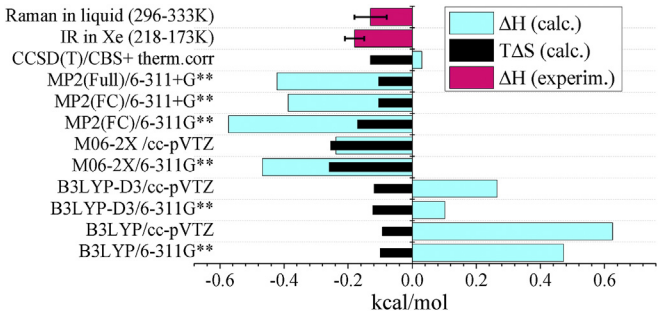

Fig. 8. Theoretical enthalpy and entropy contributions to the Gibbs energies for Eq↔Ax equilibrium computed in this works, along with CCSD(T)/CBS + therm. corr [15] and experimental data [13].

value is predicted to be −0.25 to −0.1 kcal/mol. Another situation occurs for enthalpies – essentially positive from B3LYP but negative of similar absolute value from M06-2X and MP2 approaches; moreover, |ΔH| exceeds TΔS in most of the cases, up to 5 times. Note, that coupled cluster calculations with complete basis set interpolation [15] evaluated nearly zero enthalpy. The spectroscopic data [13] on ΔH, −0.21 to −0.08 kcal/mol with experimental uncertainties taken into account, are in total smaller than their theoretical counterparts.

The GED method is sometimes applied for evaluating, in addition to structural analyses, thermodynamic data, such as oligomerization enthalpies (monomer-dimer, dimer-trimer, etc.) [39]; experiments carried out at two or more temperatures of the same specific compound vapour can clarify trends in temperature dependent change of structural parameters, see for instance [40], or shift the isomerization equilibrium [41]. In our case, an additional GED study of overheated vapour of **1** will lead to a change of conformer contribution, and thus detect a value and sign of enthalpy for the Eq↔Ax equilibrium, but, unfortunately, a temperature raise by 300° will result in just ca. 10 mol. %, as estimated from the QC data, Fig. 7, which is comparable with the experimental uncertainty.

4. Conclusion

In our recent publications, the axial-equatorial conformational preferences were discussed in terms of comparison within series of electronegative substituents (halogens F, Cl, Br, I, At and 'pseudo-halogen' cyano group) for 1-silacyclohexanes and cyanocyclohexanes [15] and within series of 1-cyano-1-heterocyclohexanes (heteroatom = N, C, Si, P) [17]. In Ref. [15], an anomalous tendency was demonstrated by the carbonitrile group in series F … At, CN as making a 'jump' towards the axial form contribution increase. The axial form fraction of 1-cyano-hetero-cyclohexanes increases in the series CNP < CNC < CNSiC < CNPhr [17].

In case cyanocyclohexane **1**, several NMR studies dated since 1960s, including the one performed in this work, resulted in a clear trend of (i) some dominating of the equatorial conformer regardless of solvent applied and (ii) increasing this domination, from 1.2:1 to 1.9:1, upon the temperature decrease, see Fig. 7. Gas-phase GED data along with theoretical B3LYP and B3LYP-D3 results perfectly coincide the condensed phase NMR observations, while the vibrational spectroscopy and M06 and MP2 data 'oppose' this.

The equatorial-to-axial transition path, as found from PES scans, run through ring inversion via *twist* configuration; the latter lies *ca.* 6 kcal/mol above the *chair* structures. Calculated energy barrier trough a semi-*twist* form of ca. 12 kcal/mol, Figs. 2 and 3, can be considered as consistent with the Gibbs energy $\Delta G^{\#}$

$_{e\rightarrow a} = 10.9 \pm 0.1$ kcal mol^{-1} which was obtained for the temperature range 185–245 K by DNMR measurements in this works.

Acknowledgments

S.A.S. is thankful to the Ministry of Education and Science of Russian Federation through Project Supporting Program (Project No. 4.3232.2017/4.6). Á.K. and I.A. are grateful to Ragnar Bjornsson for carrying out the chemical shift calculations.

Appendix A. Supplementary data

Supplementary data related to this article can be found at https://doi.org/10.1016/j.molstruc.2018.05.013.

References

[1] C. Zheng, S. Subramaniam, V.F. Kalasinsky, J.R. Durig, Raman and infrared studies supported by ab initio calculations for the determination of conformational stability, silyl rotational barrier and structural parameters of cyclohexyl silane, J. Mol. Struct. 785 (2006) 143–159, https://doi.org/10.1016/j.molstruc.2005.09.039.

[2] E. Kleinpeter, Conformational analysis of saturated heterocyclic six-membered rings, Adv. Heterocycl. Chem. 86 (2004) 41–127, https://doi.org/10.1016/S0065-2725(03)86002-6.

[3] T.D. Phien, S.A. Shlykov, N-substituted alkyl- and nonalkylpiperidines: equatorial, axial or intermediate conformations? Comput. Theor. Chem. 1087 (2016) 26–35, https://doi.org/10.1016/j.comptc.2016.04.025.

[4] E.W. Warnhoff, When piperidine was a structural problem, Bull. Hist. Chem. 22 (1998). http://www.scs.illinois.edu/~mainzv/HIST/bulletin_open_access/num22/num22 p29–34.pdf. (Accessed 3 May 2018).

[5] B.A. Shainyan, S.V. Kirpichenko, E. Kleinpeter, S.A. Shlykov, D.Y. Osadchiy, Molecular structure and conformational analysis of 3-methyl-3-phenyl-3-silatetrahydropyran. Gas-phase electron diffraction, low temperature NMR and quantum chemical calculations, Tetrahedron 71 (2015) 3810–3818, https://doi.org/10.1016/j.tet.2015.03.117.

[6] B.A. Shainyan, S.V. Kirpichenko, N.N. Chipanina, L.P. Oznobikhina, E. Kleinpeter, S.A. Shlykov, D.Y. Osadchiy, Synthesis and conformational analysis of 3-Methyl-3-silatetrahydropyran by GED, FTIR, NMR, and theoretical calculations: comparative analysis of 1-Hetero-3-methyl-3-silacyclohexanes, J. Org. Chem. 80 (2015) 12492–12500, https://doi.org/10.1021/acs.joc.5b02355.

[7] G. Rousseau, L. Blanco, Heterocyclic compounds with a silicon atom and another non-adjacent different heteroatom, Tetrahedron 62 (2006) 7951–7993, https://doi.org/10.1016/j.tet.2006.05.054.

[8] Q. Shen, R.L. Hilderbrandt, V.S. Mastryukov, Molecular structures of silacyclohexane and silacyclopentane as determined by gas phase electron diffraction, J. Mol. Struct. 54 (1979) 121–134, https://doi.org/10.1016/0022-2860(79)80061-7.

[9] A. Bodi, A. Kvaran, S. Jonsdottir, E. Antonsson, S.O. Wallevik, I. Arnason, A. V Belyakov, A.A. Baskakov, M. Holbling, H. Oberhammer, Conformational properties of 1-fluoro-1-silacyclohexane, C5H10SiHF: gas electron diffraction, low temperature NMR, temperature dependent Raman spectroscopy, and quantum chemical calculations, Organometallics 26 (2007) 6544–6550, https://doi.org/10.1021/om7008414.

[10] I. Arnason, A. Kvaran, S. Jonsdottir, P.I. Gudnason, H. Oberhammer, Conformations of silicon-containing rings. 5. Conformational properties of 1-methyl-1-silacyclohexane: gas electron diffraction, low-temperature NMR, and quantum chemical calculations, J. Org. Chem. 67 (2002) 3827–3831, https://doi.org/10.1021/jo0200668.

[11] B.A. Shainyan, S.V. Kirpichenko, D.Y. Osadchiy, S.A. Shlykov, Molecular structure and conformations of 1-phenyl-1-silacyclohexane from gas-phase electron diffraction and quantum chemical calculations, Struct. Chem. 25 (2014) 1677–1685, https://doi.org/10.1007/s11224-014-0444-0.

[12] S.A. Shlykov, B.V. Puchkov, I. Arnason, S.Ó. Wallevik, N.I. Giricheva, G.V. Girichev, Y.A. Zhabanov, 1-Methoxy-1-silacyclohexane: synthesis, molecular structure and conformational behavior by gas electron diffraction, Raman spectroscopy and quantum chemical calculations, J. Mol. Struct. 1154 (2018) 570–578, https://doi.org/10.1016/J.MOLSTRUC.2017.10.088.

[13] J.R. Durig, R.M. Ward, A.R. Conrad, M.J. Tubergen, K.G. Nelson, P. Groner, T.K. Gounev, Microwave, Raman, and infrared spectra, r0 structural parameters, conformational stability, and vibrational assignment of cyanocyclohexane, J. Mol. Struct. 967 (2010) 99–111, https://doi.org/10.1016/j.molstruc.2009.12.046.

[14] D.J. Raber, M.D. Johnston, M.A. Schwalke, Structure elucidation with lanthanide-induced shifts. 2. Conformational analysis of cyclohexanecarbonitrile, J. Am. Chem. Soc. 99 (1977) 7671–7673, https://doi.org/10.1021/ja00465a042.

[15] A.V. Belyakov, Y.F. Sigolaev, S.A. Shlykov, S. Wallevik, N.R. Jonsdottir, S. Jonsdottir, Á. Kvaran, R. Bjornsson, I. Arnason, Conformational properties of 1-cyano-1-silacyclohexane, $C_5H_{10}SiHCN$: gas electron diffraction, low-temperature NMR and quantum chemical calculations, J. Mol. Struct. 1132 (2017) 149–156, https://doi.org/10.1016/j.molstruc.2016.10.012.

[16] F.R. Jensen, C.H. Bushweller, B.H. Beck, Conformational preferences in monosubstituted cyclohexanes determined by nuclear magnetic resonance spectroscopy, J. Am. Chem. Soc. 91 (1969) 344–351, https://doi.org/10.1021/ja01030a023.

[17] S.A. Shlykov, T.D. Phien, P.M. Weber, Intramolecular inversions, structure and conformational behavior of gaseous and liquid N-cyanopiperidine. Comparison with other 1-cyanoheterocyclohexanes, J. Mol. Struct. 1138 (2017) 41–49, https://doi.org/10.1016/j.molstruc.2017.03.006.

[18] G.V. Girichev, A.N. Utkin, Y.F. Revichev, Upgrading the EMR-100 Electron-diffraction Camera for Use with Gases, vol. 27, Instruments Exp. Tech, New York, 1984, pp. 457–461.

[19] N.I. Giricheva, G.V. Girichev, S.A. Shlykov, V.A. Titov, T.P. Chusova, The joint gas electron diffraction and mass spectrometric study of GeI4(g) + Ge(s) system. Molecular structure of germanium diiodide, J. Mol. Struct. 344 (1995) 127–134, https://doi.org/10.1016/0022-2860(94)08408-A.

[20] NIST Mass Spectrometry Data Center Collection (C) 2014 copyright by the U.S., Secretary of Commerce on Behalf of the United States of America. All Rights Reserved, NIST Mass Spectrometry Data Center, 1994. NIST MS number: 135292.

[21] H.J. Reich, WinDNMR: dynamic NMR spectra for windows, J. Chem. Educ. 72 (1995) 1086, https://doi.org/10.1021/ed072p1086.1.

[22] M.J. Frisch, G.W. Trucks, H.B. Schlegel, G.E. Scuseria, M.A. Robb, J.R. Cheeseman, J.A. Montgomery Jr., T. Vreven, K.N. Kudin, J.C. Burant, J.M. Millam, S.S. Iyengar, J. Tomasi, V. Barone, B. Mennucci, M. Cossi, G. Scalmani, N. Rega, G.A. Petersson, H. Nakatsuji, M. Hada, M. Ehara, K. Toyota, R. Fukuda, J. Hasegawa, M. Ishida, T. Nakajima, Y. Honda, O. Kitao, H. Nakai, M. Klene, X. Li, J.E. Knox, H.P. Hratchian, J.B. Cross, C. Adamo, J. Jaramillo, R. Gomperts, R.E. Stratmann, O. Yazyev, A.J. Austin, R. Cammi, C. Pomelli, J.W. Ochterski, P.Y. Ayala, K. Morokuma, G.A. Voth, P. Salvador, J.J. Dannenberg, V.G. Zakrzewski, S. Dapprich, A.D. Daniels, M.C. Strain, O. Farkas, D.K. Malick, A.D. Rabuck, K. Raghavachari, J.B. Foresman, J.V. Ortiz, Q. Cui, A.G. Baboul, S. Clifford, J. Cioslowski, B.B. Stefanov, G. Liu, A. Liashenko, P. Piskorz, I. Komaromi, R.L. Martin, D.J. Fox, T. Keith, M.A. Al-Laham, C.Y. Peng, A. Nanayakkara, M. 22 Challacombe, P.M.W. Gill, B. Johnson, W. Chen, M.W. Wong, C. Gonzalez, J.A. Pople, Gaussian 09, Revision A.01, Gaussian, Inc., Pittsburgh PA, 2009.

[23] C. Peng, P.Y. Ayala, H.B. Schlegel, M.J. Frisch, Using redundant internal coordinates to optimize equilibrium geometries and transition states, J. Comput. Chem. 17 (1996) 49–56, https://doi.org/10.1002/(SICI)1096-987X(19960115)17:1<49::AID-JCC5>3.0.CO;2–0.

[24] C. Peng, H. Bernhard Schlegel, Combining synchronous transit and Quasi-Newton methods to find transition states, Isr. J. Chem. 33 (1993) 449–454, https://doi.org/10.1002/ijch.199300051.

[25] R. Ditchfield, Self-consistent perturbation theory of diamagnetism, Mol. Phys. 27 (1974) 789–807, https://doi.org/10.1080/00268977400100711.

[26] F. Weigend, R. Ahlrichs, Balanced basis sets of split valence, triple zeta valence and quadruple zeta valence quality for H to Rn: design and assessment of accuracy, Phys. Chem. Chem. Phys. 7 (2005) 3297, https://doi.org/10.1039/b508541a.

[27] (a) J. Perdew, K. Burke, M. Ernzerhof, Generalized gradient approximation made simple, Phys. Rev. Lett. 77 (1996) 3865–3868, https://doi.org/10.1103/PhysRevLett.77.3865;
(b) J.P. Perdew, K. Burke, M. Ernzerhof, Generalized gradient approximation made simple, Phys. Rev. Lett. 78 (1997) 1396, https://doi.org/10.1103/PhysRevLett.78.1396;
(c) C. Adamo, V. Barone, Toward reliable density functional methods without adjustable parameters: the PBE0 model, J. Chem. Phys. 110 (1999) 6158–6170, https://doi.org/10.1063/1.478522.

[28] F. Jensen, Segmented contracted basis sets optimized for nuclear magnetic shielding, J. Chem. Theor. Comput. 11 (2015) 132–138, https://doi.org/10.1021/ct5009526.

[29] S. Grimme, J. Antony, S. Ehrlich, H. Krieg, A consistent and accurate ab initio parametrization of density functional dispersion correction (DFT-D) for the 94 elements H-Pu, J. Chem. Phys. 132 (2010), 154104, https://doi.org/10.1063/1.3382344.

[30] N.L. Allinger, W. Szkrybalo, Conformational analysis. XXX. The cyano group [1,2], J. Org. Chem. 27 (1962) 4601–4603, https://doi.org/10.1021/jo01059a111.

[31] B. Rickborn, F.R. Jensen, The conformational preference of the cyano group [1], J. Org. Chem. 27 (1962) 4606–4608, https://doi.org/10.1021/jo01059a113.

[32] H.J. Schneider, V. Hoppen, Carbon-13 nuclear magnetic resonance substituent-induced shieldings and conformational equilibriums in cyclohexanes, J. Org. Chem. 43 (1978) 3866–3873, https://doi.org/10.1021/jo00414a017.

[33] D. Höfner, I. Tamir, G. Binsch, Dynamic proton magnetic resonance studies on complex spin systems. Non-mutual three-spin exchange inN-(trideuteriomethyl)-2-cyanoaziridine, Org. Magn. Reson. 11 (1978) 172–178, https://doi.org/10.1002/mrc.1270110404.

[34] Y.V. Vishnevskiy, Y.A. Zhabanov, New implementation of the first-order perturbation theory for calculation of interatomic vibrational amplitudes and corrections in gas electron diffraction, J. Phys. Conf. Ser. 633 (2015) 012–076, https://doi.org/10.1088/1742-6596/633/1/012076.

[35] A.E. Aliev, K.D.M. Harris, Conformational properties of monosubstituted

cyclohexanes in their thiourea inclusion compounds and in solution: variable-temperature one-dimensional and two-dimensional carbon-13 NMR investigations, J. Am. Chem. Soc. 115 (1993) 6369–6377, https://doi.org/10.1021/ja00067a061.

[36] H. Booth, J.R. Everett, R.A. Fleming, Carbon-13 magnetic resonance studies of cyclic compounds. 2. Carbon-13 chemical shift parameters for equatorial and axial substituents in cyclohexane: the substituents methyl, ethyl, isopropyl, methoxy and phthalimido, Org. Magn. Reson. 12 (1979) 63–66, https://doi.org/10.1002/mrc.1270120204.

[37] H.-O. Kalinowski, S. Berger, S. Braun, Die Chemische Verschiebung, 13C NMR Spektrosk, 1984, pp. 77–419.

[38] K. Pihlaja, E. Kleinpeter, Carbon-13 NMR Chemical Shifts in Structural and Stereochemical Analysis, VCH Publishers, Inc, New York, 1994.

[39] S.A. Shlykov, Y.A. Zhabanov, N.I. Giricheva, A.G. Girichev, G.V. Girichev, Combined gas electron diffraction/mass spectrometric study of beryllium diiodide assisted by quantum chemical calculations: structure and thermodynamics of beryllium dihalides, Struct. Chem. 26 (2015) 1451–1458, https://doi.org/10.1007/s11224-015-0614-8.

[40] A.V. Titov, G.V. Girichev, N.I. Girichev, S.A. Shlykov, S.V. Smorodin, Electron-diffraction and Quantum-chemical Studies of the Temperature Dependence of the Structural Parameters of the TiCl4 Molecule in the Temperature Range from 0 ° C to 600 ° C, Izvestiya Vysshikh Uchebnykh Zavedeniy, Seriya “Khimiya I Khimicheskaya Tekhnologiya”, vol. 51, 2008, pp. 68–72.

[41] N.V. Belova, H. Oberhammer, N.H. Trang, G.V. Girichev, Tautomeric properties and gas-phase structure of acetylacetone, J. Org. Chem. 79 (2014) 5412–5419, https://doi.org/10.1021/jo402814c.